

Behaviour of Deep Embedded FRP/Steel bars

Vesna Raicic¹, Tim Ibell², Antony Darby³, Mark Evernden⁴ and John Orr⁵

¹Early Stage Researcher at the University of Bath, Bath, United Kingdom

²Professor and Associate Dean (Research) at the University of Bath, Bath, United Kingdom

³Dr. Reader in Structural Engineering at the University of Bath, Bath, United Kingdom

⁴Dr. Lecturer at the University of Bath, Bath, United Kingdom

⁵Dr. Lecturer at the University of Bath, Bath, United Kingdom

ABSTRACT: This paper describes shear capacity and failure mechanisms of reinforced concrete push-off specimens strengthened with deep embedded FRP/Steel bars across a shear plane. An emphasis was put on the minimum bar anchorage lengths required for effective shear transfer. For this purpose, ten initially uncracked push-off specimens were designed to fail along a known shear plane. Four specimen types were strengthened using CFRP, GFRP and steel bars of 10mm diameter respectively. These bars crossed the shear plane at an angle of 45° and 90° with varying anchorage lengths and constant reinforcement ratio of 0.26% in order to examine their effect on shear friction capacity more closely. Therefore, this paper reports on the test results, and on their significance in being able to apply deep embedment strengthening techniques to concrete structures.

1 INTRODUCTION

Due to light weight, high tensile strength and ease of installation, the use of Fibre-Reinforced Polymer (FRP) materials has become a widely accepted practice within the civil engineering world, especially in the rehabilitation of existing reinforced concrete (RC) structures, (Belarbi et al. 2013). The most commonly used configuration schemes for increasing shear capacity of continuous T-beams, where accessibility is not an issue, are side, U or full wrapping with FRP composite sheets. But in reality T-beams are frequently cast monolithically with the top slab in which case full wrapping is not a feasible option, (Belarbi 2013; Ahmad et al. 2012). A recently developed technique for strengthening RC beams in shear using FRP bars (Deep Embedment-DE or Embedded Through Section-ETS) has proven to be superior in comparison with Externally Bonded (EB) and Near Surface Mounted (NSM) methods (Valerio et al. (2003); Mofidi et al. (2012)). This technique involves inserting FRP or steel bars upwards into vertical holes which have been drilled from the soffit of concrete beams, thus connecting the top and bottom chords.

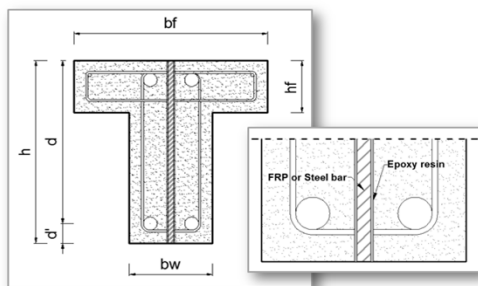


Figure 1. Deep Embedment technique

Since DE is a fairly new technique, more research needs to be conducted on behaviour of deep embedded bars and the extent to which these bars are capable of transferring shear stresses across a known shear plane. In order to do that, it is necessary to isolate parameters that can affect this shear-strengthening system. Birkeland and Birkeland (1966) carried out tests on initially uncracked steel reinforced push-off specimens to develop a shear friction hypothesis. This approach was further developed by Hofbeck et al. (1969), Mattock et al. (2001) and Walraven (1981) on both cracked and uncracked specimens. Investigation of shear capacity of concrete reinforced with FRP materials has also been done in order to determine its efficiency, (Ibell and Burgoyne, 1999). More recently, Grusova et al. (2013) have studied the effectiveness of FRP sheets on the resistance to shear in steel reinforced concrete by using push-off specimens.

Therefore, it is of great importance to deepen our understanding of failure mechanisms in DE strengthened steel reinforced concrete as well as the contribution of FRP/steel bars to the total shear friction capacity. This is especially true given that it has been proven that the assumption (accepted by current design codes) of simply summing the contributions to shear resistance from concrete, steel and FRP is unrealistic in its application (Grusova et al. 2013).

2 EXPERIMENTAL PROGRAM

For this experimental campaign, 10 initially uncracked push-off specimens were tested. They were classified into four categories depending on the type, anchorage length and angle of insertion of the bars. An emphasis was placed on the minimum bar anchorage lengths required for effective shear stress transfer.

2.1 Description of the specimens

Figure 1 represents the size of a typical push-off specimen, 300mm thick, 200mm wide and 660mm high. They were all cast with constant shear plane area of 200mm x300mm. Each specimen consisted of two non-symmetrical parts, monolithically connected, reinforced with steel cages assembled of 12 B500B steel L-bars with diameter of 16mm. Bars were positioned and fixed with steel stirrups of diameter 8mm which were not placed through the shear plane, so as not to influence the result. Steel cages were intentionally placed away from the shear plane in order to avoid unwanted failure modes.

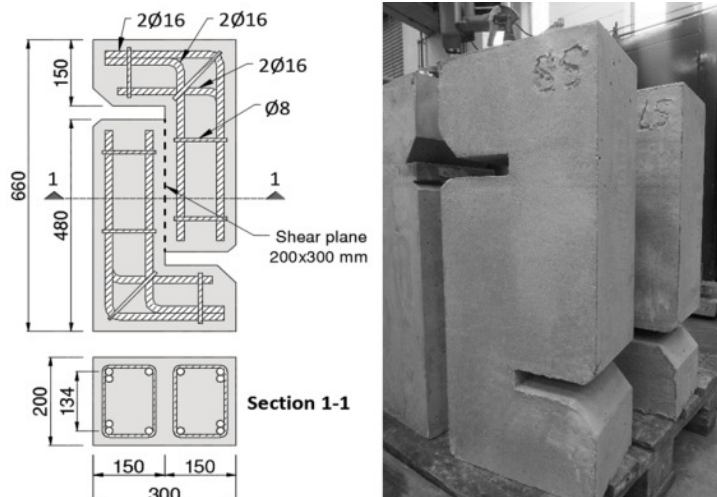
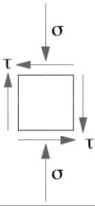


Figure 1. Steel reinforcement of the specimens and their appearance after casting

Dimensions of the specimens were adopted concerning the average geometry of typical continuous reinforced concrete beams in buildings, cast monolithically with the top slab. Nevertheless, they were designed in the way that the shear-to-normal stress ratio was constant throughout the entire test process in order to be able to compare the results of different strengthening schemes, see Table 1. As previously done by other researchers (Hofbeck and Mattock, 1969), these push-off specimens were also intended to fail along a known plane so that it was possible to isolate numerous shear influences.

Table 1 Determination of shear to normal ratio

	$\sigma = C_{\sigma} \frac{2P}{Lb}$	- Normal stress	(1)	P –axial compressive load
	$\tau = C_{\tau} \frac{P}{bh}$	- Shear stress	(2)	$C_{\sigma} = C_{\tau} = 1$ assumed uniform distribution of the stresses
	$k = \frac{\tau}{\sigma} = \frac{L}{2h} = 0.5$	- Shear to normal stress ratio	(3)	L/2 – width of the loading plate

2.2 Materials used

All ten push-off specimens were cast in the University laboratory. Each batch provided 2 test specimens, 4 cubes and 3 cylinders. Cubes of 100x100x100mm were used for determination of compressive cube strength after 7, 14, 28 days and on the day of testing. To verify tensile splitting strength 3 cylinders 100mm in diameter and 200mm high were tested after 7 and 28 days and on the day of testing. Average values from standard cube and tensile splitting tests showed $f_{cu} = 60\text{MPa}$ for concrete compressive strength and $f_{ct} = 3.76\text{MPa}$ for concrete tensile strength. It was important to design a concrete mix with good workability, especially due to closely-spaced reinforcing bars. Since repeatability of concrete mix was important for accurate test results, great care was taken when mixing all of the ingredients.

Spirally wound sand-coated FRP reinforcing bars were used for specimen strengthening together with two-component adhesive. Their properties are given in Table 2.

Table 2. Characteristic material properties

Material	Tensile strength f_{tu} (MPa)	Modulus of elasticity E_f (GPa)	Ultimate strain (%)
Aslan 200 CFRP bar	2172	124	1.75
Aslan 100 GFRP bar	827	46	1.79
Steel bar	500	210	/
Hilti HIT-RE500 Epoxy resin	43.5	1.49	2.00

2.3 Test setup and instrumentation

As illustrated in Figure 2, specimens were placed between a hydraulic actuator and the reaction frame of the hydraulic test rig which has a capacity of 200t. They were subjected to axial compressive load at a rate of 0.2 mm/min in order to produce direct shear along the shear plane. It was very important to avoid inadmissible failure modes and buckling patterns outside the fracture plane. For this purpose two steel plates were placed at the top and bottom of the specimens to prevent compressive stress concentration. These plates were 200mm long, 15mm thick and 150mm wide.

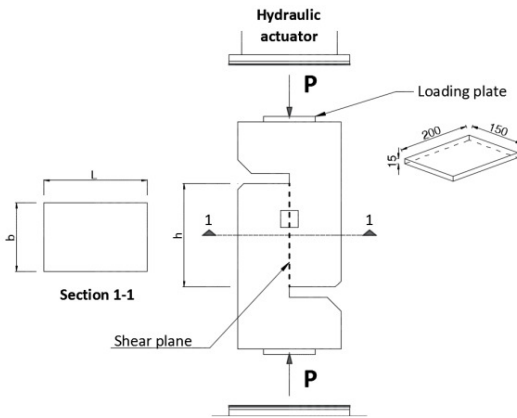


Figure 2. Test setup

In order to measure vertical displacement (shear) two linear variable differential transformers (LVDTs) were placed on both sides of the specimens as schematically shown in Figure 3. The same was done for measuring horizontal displacement (crack opening). One diagonal and one horizontal LVDT were placed at the location of deep embedded bars.

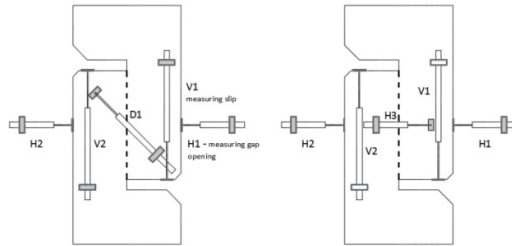


Figure 3. Positions of LVDTs

2.4 Specimen strengthening

All specimens were divided into four categories depending on the bar type and angle of its insertion. Type I specimens were strengthened with CFRP bars of variable anchorage lengths, all inserted at an angle of 45° relative to the shear plane. Type II specimens were also strengthened with CFRP bars of different anchorage lengths but inserted perpendicular to the shear plane. Type III and Type IV were strengthened as Type I but with use of GFRP and Steel bars. Each of the nine specimens was strengthened with bars of diameter 10mm and their characteristics are listed in Table 3.

Table 3. Four types of specimens

Specimen type	Mark	Bars			Anchorage length l [mm]
		Type	d [mm]	ρ [%]	
O	CON	/	/	/	/
I	C100	CFRP	10	0.26	100
I	C150	CFRP	10	0.26	150
I	C200	CFRP	10	0.26	200
II	C75h	CFRP	10	0.26	75
II	C150h	CFRP	10	0.26	150

III	G100	GFRP	10	0.26	100
III	G200	GFRP	10	0.26	200
IV	S100	Steel	10	0.26	100
IV	S200	Steel	10	0.26	200

Assuming that the shear discontinuity develop at an angle of approximately 45° with respect to the horizontal beam axis, the 45° and 90° push-off geometries were chosen to investigate vertical and inclined Deep Embedded bars, respectively, see Figure 4.

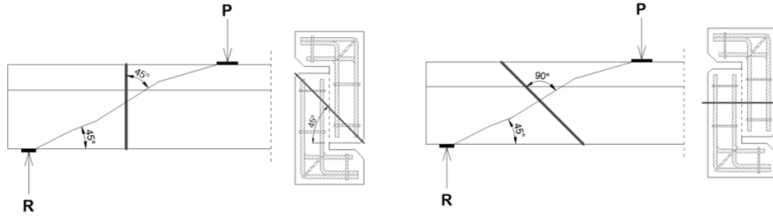
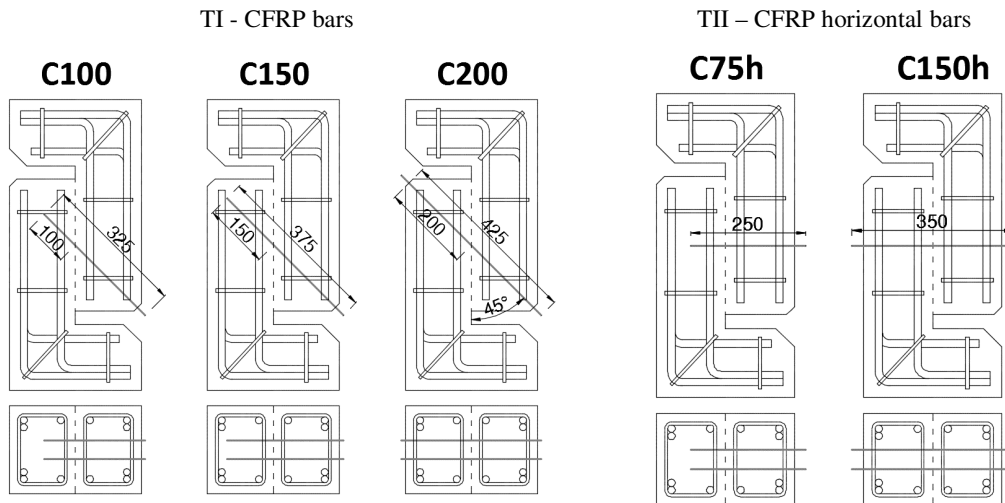


Figure 4. Different angles of bar insertion

Two holes of diameter 14mm were drilled from the side of the specimens, leaving a space of 2mm around the bars to ensure a sufficient thickness of the adhesive layer and thus good bond between concrete and bars. Two strain gauges were placed on the opposite sides of the bars at the shear plane. After drilling the holes, dust was removed with compressed air and two-component epoxy inserted. The bars were then slowly pushed into the holes in order to avoid formation of air bubbles. Figure 5 provides details of each specimen geometry and anchorage length.



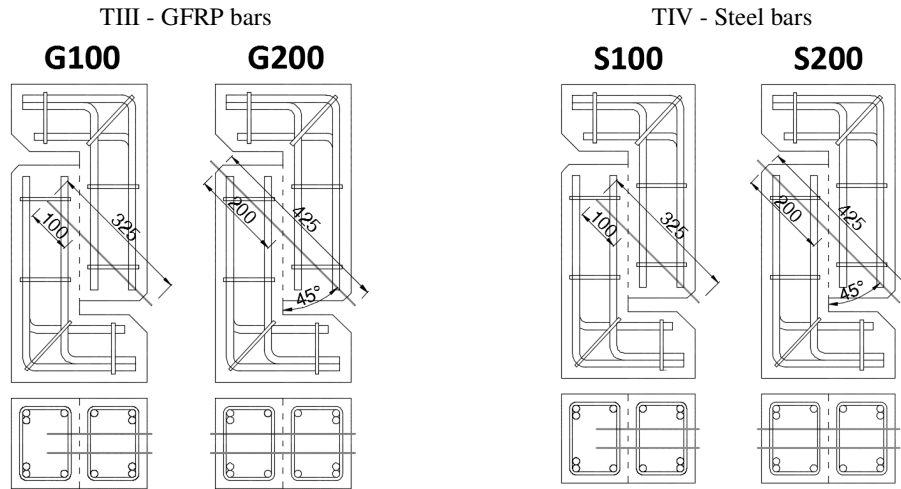


Figure 5. Specimen details

3 PREDICTIONS OF SPECIMENS SHEAR CAPACITY

3.1 Analysis approach

Hofbeck and Mattock (1969) performed several tests on both uncracked and cracked push-off specimens to obtain the relationship between normal and shear stresses acting along the shear plane, basing their analysis on shear friction theory. When applying axial compressive force on the specimens a crack is formed along the shear plane with rough and irregular faces. The two halves will tend to separate when slip occurs, putting the bars crossing the shear plane into tension. This will on the other hand create a compressive stress in the concrete along the shear plane that will provide the resistance to slip, see Figure 6.

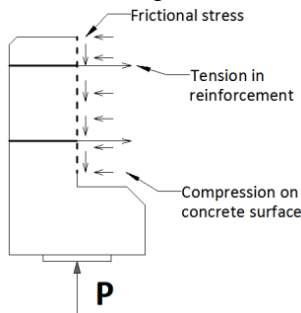


Figure 6. Shear-friction model

Since bond strength and stiffness of the bars play an important role in transferring the load, this analytical approach is also based on the work done by Walraven (1981) who established relationships amongst normal stress, shear stress, shear slip and width of the crack, extended by Ibell and Burgoyne (1999). Considering that Walraven's work was based on precracked specimens, initial strength of the specimens cannot be predicted by this approach but rather the post peak plateau, cohesion is ignored, see Figure 7.

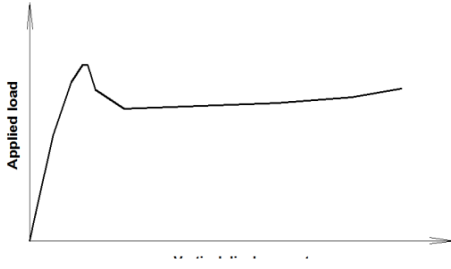


Figure 7. Typical load/vertical displacement diagram for specimens reinforced with FRP bars

Accordingly, this prediction will consist of:

- Assuming the bond strength of deep embedded bars based on previous bond tests (Valerio et.al 2009).
- Assuming the crack width when plateau behaviour is reached
- Using Walraven's analysis to calculate vertical slip and shear stress
- Calculating the predicted capacity of the specimens.

Based on this, following equations are used:

- Debonding length $l_d = \frac{F_b}{\sigma_b l_p}$ (4)

- Crack width $w = \frac{F_b l_d}{2AE} \rightarrow w = \frac{F_b^2}{2\sigma_b l_p AE}$ (5)

- Maximum force in the bar $F_b = \sqrt{2w\sigma_b l_p AE}$ (6)

- Normal stress $\sigma = \frac{2 * F_b}{bh}$ (7)

- Normal stress $\sigma_{ncr} = -\frac{f_{cu}}{20} + [1.35w^{-0.63} + (0.191w^{-0.552} - 0.15)f_{cu}]s$ (8)

- Shear stress $\tau_{cr} = -\frac{f_{cu}}{30} + [1.8w^{-0.8} + (0.234w^{-0.707} - 0.20)f_{cu}]s$ (9)

- Predicted specimens capacity $P = \tau bh$ (10)

Key: l_d -debonding length, F_b -maximum force in the bar, σ_b -bond strength, l_p -perimeter of bar cross section, w -crack width, A -nominal area of the bar, E -tensile modulus of elasticity, f_{cu} -compressive strength of the concrete, s -vertical slip

4 RESULTS

Results from these predictions are listed in Table 4, assuming the following parameters:

Bond strength for GFRP bars: $\sigma_b = 16$ MPa, CFRP bars: $\sigma_b = 20$ MPa, STEEL bars: $\sigma_b = 20$ MPa

Crack width: $\omega = 0.5$ mm

Table 4. Predicted capacity of the specimens

	Specimen	P_u (kN)
1	CON	225
2	G100	275

3	G200	275
4	S100	283
5	S200	283
6	C75h	347
7	C150h	347
8	C100	390
9	C150	390
10	C200	390

Note: Given that testing has not yet been carried out, test results, failure modes and explanations will be presented in detail at the conference special session on “Presentation Competition for Early Stage Researchers”

5 CONCLUSIONS

This paper has presented details of a testing system to be used to determine the anchorage requirements for FRP and steel bars when placed vertically or at an inclination in a Deep Embedment strengthening strategy. Test results to be presented at the conference will confirm or deny the predicted capacities outlined in this paper.

6 ACKNOWLEDGEMENTS

The authors gratefully acknowledge the help of the laboratory staff of University of Bath and Marie Curie Initial Training Network - endure (European Network for Durable Reinforcement and Rehabilitation Solutions).

7 REFERENCES

- Ahmad, Saeed, et al. "Shear strengthening of reinforced concrete continuous beams." *Proceedings of the ICE-Structures and Buildings* 166.5 (2012): 247-256.
- Belarbi, Abdeldjelil, and Bora Acun. "FRP systems in shear strengthening of reinforced concrete structures." *Procedia Engineering* 57 (2013): 2-8.
- Birkeland, Philip W., and Halvard W. Birkeland. "Connections in precast concrete construction." *ACI Journal Proceedings*. Vol. 63. No. 3. ACI, 1966.
- Grusova, Monika, et al. "Mechanics of failure in FRP strengthened reinforced concrete in shear." *The Fourth International fib Congress*. University of Bath, 2014.
- Hofbeck, J. A., I. O. Ibrahim, and Alan H. Mattock. "Shear transfer in reinforced concrete." *ACI Journal Proceedings*. Vol. 66. No. 2. ACI, 1969.
- Ibell, Tim, and Chris Burgoyne. "Use of fiber-reinforced plastics versus steel for shear reinforcement of concrete." *ACI Structural Journal* 96.6 (1999).
- Mattock, Alan H. "Shear friction and high-strength concrete." *ACI Structural Journal* 98.1 (2001).
- Mofidi, Amir, et al. "Experimental tests and design model for RC beams strengthened in shear using the embedded through-section FRP method." *Journal of Composites for Construction* 16.5 (2012): 540-550.
- Valerio, Pierfrancesco and Timothy James Ibell. "Shear strengthening of existing concrete bridges." *Proceedings of the ICE-Structures and Buildings* 156.1 (2003): 75-84.
- Walraven, J. C., and H. W. Reinhardt. "Theory and experiments on the mechanical behaviour of cracks in plain and reinforced concrete subjected to shear loading." *HERON*, 26 (1A), 1981 (1981).